IMPORTANCE OF SAMPLING DESIGN TO INCREASE CLIMATE SIGNAL DETECTION IN SHRUB RING CHRONOLOGIES

Tania Pereira, Loïc Francon, Christophe Corona and Markus Stoffel

With 7 figures and 2 tables
Received 26 January 2023 · Accepted 10 February 2023

Summary: Shrub dendrochronology is gaining increasing momentum in temperate high mountain regions to decipher climatic controls on current shrub expansion. Yet, a lack of consensus still persists in terms of sampling protocols, thus hampering comparability of results from different studies. For instance, serial sectioning, i.e. the sampling of multiple sections along the same shrub stem is recommended as it increases the detection of partial and missing rings, but has only been employed in few studies as it is time-consuming. Similarly, as a result of serial sectioning, chronologies frequently combine sections sampled at different positions along the stem and at the root collar which hinders the detection of climatic signals. Here, we used cross-sections sampled on 21 *Rhododendron ferrugineum* shrubs from the French Pyrenees to define a parsimonious protocol enabling detection of partial and missing rings while increasing the strength of the climate signal in the shrub ring chronology. We demonstrate that partial and missing rings are almost evenly distributed along *Rhododendron ferrugineum* stems and that they can be detected optimally using two sections on which growth rings are measured along three radii. Our results also evidence that chronologies which include only ring-width series from basal sections more strongly integrate summer temperature fluctuations than stem-based or mixed chronologies. Noteworthy, the snowpack signal is stronger in chronologies with individuals from the upper stem sections. Overall, our results confirm that sampling design - serial sectioning and caution in ring-width series aggregation - is key to ensure robustness of dendroecological studies on dwarf shrubs in alpine environments.

Zusammenfassung: Die Dendrochronologie von Sträuchern gewinnt in gemäßigten Hochgebirgsregionen zunehmend an Bedeutung, um die klimatischen Einflüsse auf die aktuelle Ausbreitung von Sträuchern zu entschlüsseln. Dennoch fehlen nach wie vor Standards hinsichtlich der Probennahme, was die Vergleichbarkeit der Ergebnisse verschiedener Studien erschwert. So wird z. B. das ‚serial sectioning', d. h. die Beprobung mehrerer Abschnitte entlang desselben Strauchstamms, empfohlen, da es die Erkennung partieller und fehlender Ringe erhöht, es wurde bisher aber nur in wenigen Studien angewandt, da es sehr zeitaufwändig ist. Ebenso werden bei Chronologien aufgrund der seriellen Schnittführung häufig Abschnitte kombiniert, die an verschiedenen Positionen entlang des Stammes und am Wurzelhals entnommen wurden, was die Erkennung von Klimasignalen erschwert. Hier haben wir Querschnitte von 21 *Rhododendron ferrugineum* Sträuchern aus den französischen Pyrenäen verwendet, um ein einfaches Protokoll zu erarbeiten, das die Erkennung von partiellen und fehlenden Ringen ermöglicht und gleichzeitig die Stärke des Klimasignals in der Strauchringchronologie erhöht. Wir zeigen, dass partielle und fehlende Ringe fast gleichmäßig über die Stämme von *Rhododendron ferrugineum* verteilt sind und dass sie optimal mit zwei Abschnitten erfasst werden können, an denen Wachstumsringe entlang dreier Radien gemessen werden. Unsere Ergebnisse zeigen auch, dass Chronologien, die nur Ringbreitenreihen aus basalen Abschnitten enthalten, die sommerlichen Temperaturschwankungen stärker integrieren als stammbasierte oder gemischte Chronologien. Bemerkenswert ist, dass das Schneedeckensignal in Chronologien mit Individuen aus den oberen Stammabschnitten stärker ist. Insgesamt bestätigen unsere Ergebnisse, dass das Stichprobendesign - serielle Schnitte und eine vorsichtige Aggregation von Ringbreitenreihen - der Schlüssel zur Gewährleistung der Robustheit dendroökologischer Studien an Zwergsträuchern in alpinen Umgebungen ist.

Keywords: Alpine shrubs, dendroecology, methodology, *Rhododendron ferrugineum*, climate sensitivity, Pyrenees

1 Introduction

High-altitude and high-latitude environments are experiencing more pronounced warming than the rest of the globe (IPCC 2021). As a result, alongside rising temperature, vegetation surveys have shown widespread shrub expansion (shrubification) and increasing productivity (greening) which in turn were shown to modify a wide range of ecological processes in arctic and alpine tundra ecosystems (Chapin et al. 2005, Liston et al. 2002, Myers-Smith et al. 2020, Sturm et al. 2001). Dendroecological studies, relying on precisely dated annual rings of woody plants to study (multi-)decadal changes in ecological systems, have consequently gained considerable momentum in alpine tundra ecosystems

https://doi.org/10.3112/erdkunde.2022.04.04 ISSN 0014-0015 (Print) · ISSN 2702-5985 (Online)

over the last two decades (Bär et al. 2008, Dobbert et al. 2022, Hallinger et al. 2010, Hallinger & Wilmking, 2011, Moullec et al. 2019, Myers-Smith et al. 2011, Tape et al. 2012, Weijers et al. 2010, Wilmking et al. 2012, Schweingruber & Poschlod 2005, Weijers et al. 2018a, 2018b). However, shrub dendroecology presents methodological challenges. Growth deformities such as reduced stem diameters, scarring, multi-stems, frequent eccentric secondary growth, and considerable heterogeneity in growth (and associated irregularities in ring growth) within and between individuals (Moullec et al. 2019, Myers-Smith et al. 2015b) are common in alpine shrubs. They can lead to (partially) missing rings, which can be caused by limited resource availability (Hallinger et al. 2010), cambial age (Wilmking et al. 2012), but also by climatic extremes such as cold and short growing seasons (Buchwal et al. 2013) or frost damage to the cambium (Bär et al. 2006, Myers-Smith et al. 2015b).

Therefore, the dendroecological protocol has been adapted in various ways to consider the morphology of dwarf shrubs. Methodological adjustments were made in sampling procedures and preparation techniques (Moullec et al. 2019, Myers-Smith et al. 2015b), with cross-sections systematically preferred over increment cores (Buras & Wilmking, 2014) and micro-sections preferred over sanding and polishing (Schweingruber & Poschlod 2005). At the scale of individual shrubs, the recommended sampling method in shrub dendrochronology is serial sectioning (Kolishchuk 1990), i.e. taking several sections at multiple points along a stem from a given individual to allow multilevel cross-dating (Bär et al. 2008, Buchwal 2014, Wilmking et al. 2012). Although the suitability of this sampling strategy for the detection of (partially) missing or rings is undeniable, Ropars et al. (2017) and Shetti et al. (2018) demonstrated in the Arctic and in the Ural mountains that climatic signals are better preserved in growth rings taken at the root collar. They thus concluded that the selection of shrub stem cross-sections is crucial for climate sensitivity analyses. Yet, these studies have been limited to two shrub species – i.e., *Betula glandulosa* and *Juniperus communis* – and complementary investigations are thus needed to determine the extent to which these findings are transferable to other species. In particular, in the European Alps, where studies are scarcer than in the Arctic, no clear guidelines have been proposed so far on sampling strategies that would maximize the signal–noise ratio in dendroecology applied to shrubs.

For this reason, this study focuses on two research questions. We first tested the added value of multiple radial measurements to detect partial rings and of the serial sectioning sampling approach to detect missing rings in a multi-stemmed shrub species. In a second step, we checked the consistency of the dendrochronological signal along and among stems and potential variations in the sensitivity of the different parts of shrubs to climate. We chose *Rhododendron ferrugineum* (L.) to answer these questions as it is one of the most widespread, multistemmed, alpine shrub species in western Europe and has been recently used in dendroecological studies in the Alps (Francon et al. 2017, 2020a) and the Pyrenees (Francon 2023).

2 Material and methods

2.1 Study site

The study site (42°45'41"N, 1°25'27"E, Fig.1) is located in the French Pyrenees, 95 km south of Toulouse (Fig 1. A, B), in the hanging valley of Bassiès, one of the main sub-basins of the Upper Vicdessos valley (1156-2679 m asl, median elevation: 1676 m, Fig. 1C). The drainage basin of the Bassiès valley (15 km^2) is composed of granitic *roches moutonnées* from the last glacial maximum (Delmas et al. 2011) forming a contrasted relief: whereas steep slopes delimit the watershed, the valley bottom is rather flat and exhibits gentle slopes in its central part (Marti et al. 2016, Simonneau et al. 2013). The catchment is mainly covered by subalpine meadows and dwarf shrubs (65%) as well as vegetation-free rock and bare soil surfaces (25%) (Marti et al. 2016, Szczypta et al. 2014). Forest and shrubby vegetation occupy 5% and 2% of the valley surface, respectively. Successional processes involving tree and shrub encroachment of open surfaces are now occurring rapidly over the catchment (Galop et al. 2011). According to the Safran-Crocus dataset (Durand et al. 2009), average annual, June-August and December-April temperatures in the area were 5.4°C, 11.4°C and 1.2°C, respectively, over the period 1981-2010. Over the same period, mean annual precipitation was 1245 mm (Fig. 1D). Average maximum snowpack depth was 91 cm (±30 cm). The snow season generally started in November–December and the snowpack melt-out date occurred around May 10. on average. Yet, over the period 1971-2019, we observe earlier snowpack melt-out dates (4 days.decade^{-1}) as well as increasing summer (June-August) and winter (December-April) temperatures (0.026 °C.year^{-1} and 0.008 °C.year^{-1}, respectively).

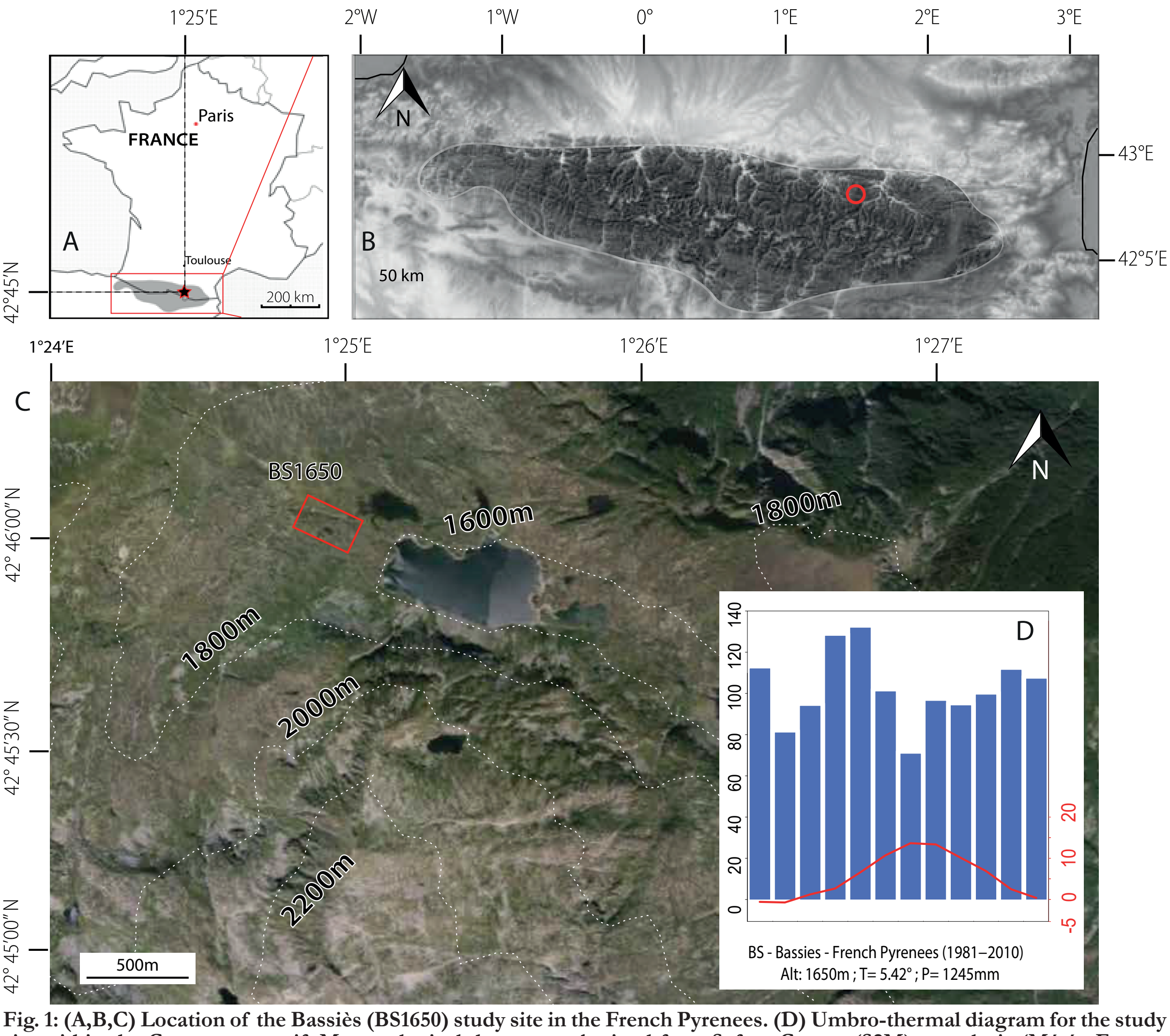

Fig. 1: (A,B,C) Location of the Bassiès (BS1650) study site in the French Pyrenees. (D) Umbro-thermal diagram for the study site within the Couseran massif. Meteorological data were obtained from Safran-Crocus (S2M) reanalysis (Météo France, 1981–2010).

2.2 Sample collection and preparation

R. ferrugineum is one of the most widespread shrub species in the Bassiès valley. This multi-stemmed dwarf shrub reaches 70 cm in height and forms large heathlands, colonizing grazed or abandoned grasslands on north-, west-, and northwest-facing slopes of the European Alps, Apennines and Pyrenees (Escaravage et al. 1998). Recent dendroecological studies (Francon et al. 2017, 2020a, 2020b, 2021, Piccinelli et al. 2023) have demonstrated the potential of *R. ferrugineum* rings as a robust proxy for the documentation of alpine vegetation response to global warming (Francon et al. 2020b). Because *R. ferrugineum* spreads by clonal propagation, the stems are burrowed and develop adventitious roots. This morphology makes it difficult to identify the oldest stem and the root-stem interface. In this study, we positioned root collar at the level of the first layer of adventitious roots. In October 2019, we randomly selected 21 individuals (BS01 to BS21, Fig. 2A) growing at an elevation of ~1650 m asl, in a rather flat and topographically homogeneous area located in the valley bottom where shrubs are colonizing grasslands (Fig. 1D). From each specimen, sections were systematically cut at the root collar (A section) and at 30 cm above the soil surface (B section). For four of these individuals (hereafter: ind$_{A\text{-}D}$, Fig. 2A), we extended sampling to two stems to cut four to seven cross-sections per stem from base to tip with the purpose to explore partial and missing ring repartition along the stems. To ensure precise detection of all rings, a total

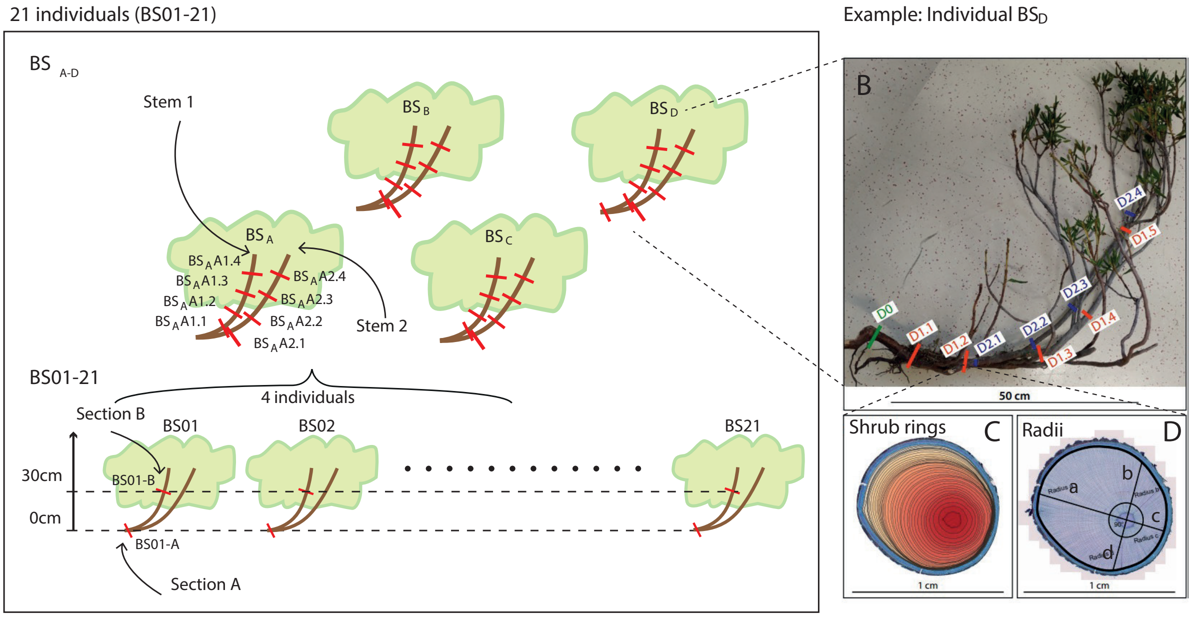

Fig. 2: (A) Sampling design: 21 individuals (BS01 to BS21) were sampled. For 17 individuals, two sections were cut at the shrub base (A section) and at 30 cm above the soil surface (B section). For four individuals (Ind_{A-D}: BS_A, BS_B, BS_C and BS_D), we sampled two main stems from which we cut four to seven cross-sections. (B) Serial sectioning of the D individual along two stems. (C) Ring area measurement. (D) location of the four measured radii (a, b, c and d) in one section.

of 75 stem sections were cut with a rotary microtome (Leica, Heidelberg, Germany) and prepared according to the wood anatomy protocol by Francon et al. (2020a). Microsections were then scanned using a D-sight 2.0 System (Menarini Diagnostics, Florence, Italy).

2.3 Crossdating and detection of missing and partial rings

For each cross-section of ind_{A-D}, we quantified annual radial growth by measuring ring widths at 4 orthogonally distributed radii (a, b, c and d), where a and c are the longest and the shortest radii, respectively (Fig. 2D). For the crossdating of the ring-width series, we used the three-step procedure described by Shetti et al. (2018) and Francon et al. (2020a). The latter consists of visual comparisons and correlations of raw ring-width series (1) from the four radii of a given cross-section, (2) from the different cross-sections sampled from the same stem and (3) between individuals. After cross-dating, we computed a missing ring (MR) rate corresponding to the ratio between the number of missing rings and the age of the cross-section for each cross-section of ind_{A-D}. We then plotted this rate as a function of section height to visualize the evolution of the MR rate along each stem. We also calculated the percentage of missing rings in the base section by dating additional sections along the stem with the idea to determine the minimum number of additional sections required for serial sectioning and to place them along the stem. For each section of ind_{A-D}, we carefully digitized ring boundaries (Fig. 2C) using a Geographic Information System software, Q-GIS, (QuantumGIS, version 3.10 A Coruña), thereby making sure to detect all rings. In a next step, we compared the total number of rings to the number of rings detected along different combinations of one, two, and three radii among radii a-d (Fig. 2D) with the aim to quantify the number of partial rings remaining undetected in different methods.

2.4 Chronology development

To remove age-related trends and non-climatic signals from the raw ring-width series from the 21 individuals, we used the dplR package (Bunn, 2008) for R software (R Core Team 2016). We applied a cubic smoothing spline with a 50% frequency response at 25 years (Cook & Peters 1981). Indexed series were then averaged into three reference chronologies using a bi-weighted robust mean to reduce the influence of outliers (Cook & Peters 1981). In order to explore the evolution of tree-ring sensitivity along branches, chronology A includes exclusively shrub cross-sections sampled at root collar (0 cm), whereas chronology B only includes shrub cross-sections sampled at 30 cm above the soil surface. The composite chronology AB includes all cross-sections sampled at 0 and 30 cm, as commonly done in most dendroecological studies applied to shrubs. Descriptive statistics including standard deviation (SD), mean sensitivity (MS), and autocorrelation (AC) were computed using the R (R Core Team 2016) dplR package (Bunn, 2008) for the three chronologies A, B and AB. In addition, the subsample signal strength, the expressed population signal (SSS and EPS; Wigley et al. 1984, Buras 2017) and mean inter-series correlation (rbar) were computed using dplR to evaluate their robustness. The SSS and EPS statistics quantify the strength of the common climate signal in the tree-ring proxies by calculating how well a finite subsample represents a finite (SSS) or infinite (EPS) sample (Buras 2017, Wigley et al. 1984). We chose a SSS threshold > 0.8 to determine the period over which each chronology is reliable to compute climate-growth analyses.

2.5 Climate sensitivity along shrubs stems

To test for the potential variability of the climate signal along shrub stems, we computed bootstrapped correlation functions (BCFs) between the detrended chronologies A, B and AB and monthly climatic variables using the R (R Core Team 2016) Treeclim package (Zang & Biondi 2015). In detail, the climatic dataset includes average monthly mean, minimum, maximum temperature and monthly precipitation totals from May of the year preceding growth-ring formation (n−1) to September of the year of actual ring formation (n), as well as snowpack variables extracted from the Safran-crocus reanalysis dataset (Durand et al. 2009, Vernay et al. 2022, Vionnet et al. 2012). Safran combines *in situ* meteorological observations with synoptic-scale meteorological fields to provide continuous time series of meteorological variables at hourly resolution. Simulations are made over elementary areas, referred to as massifs (Couserans in the case of this study), designed to represent the main drivers of the spatial variability observed in mountain ranges (elevation bands of 300 m, different slope aspects and angles) (Vernay et al. 2022). From the daily snowpack dataset, we extracted melt-out dates (defined as the last day when snow cover reached 5cm above the soil surface) and mean snowpack depth in January-February.

To further assess differences in climate sensitivity between chronologies A and B, we also used a linear mixed effects model (LMM). Following Ropars et al. (2017), we calculated a LMM with ring width index (RWI) as the response variable and the significant monthly climate variables detected in the BCF analysis, as well as sample type (A or B) as interactive predictors and year as random effect. To prevent any effect of multicollinearity among explanatory variables, we used variance inflation factors (VIF). Collinearity was assessed with a cut-off value of 4 (Zuur et al. 2010). We computed pseudo-R^2 comprising marginal (R^2m) and conditional (R^2c) values (Nakagawa & Schielzeth 2013) using MuMIn package (Bartoń 2019). R^2m and R^2c account for the proportions of the variance explained by the fixed factors and by the whole model (i.e. fixed plus random factors), respectively. To compare chronologies A and B, we performed BCFs and LMMs over a common time window for which both chronologies exceed the SSS >0.8 threshold.

3 Results

3.1 Chronology quality

A total of 15 individuals were included in the three *R. ferrugineum* chronologies corresponding to rejection rates (i.e. the percentage of misdated individuals) of 29%. BS1650A (only base sections) and AB (composite chronology) span the period 1971-2019. BS1650B (only 30cm above soil surface sections), composed of sections sampled on younger stems only dates back to 1991 (Fig. 3). The rbar and EPS statistics (Tab. 1), computed on spline detrended chronologies, are comparable, in the range 0.19-0.25 (rbar) and 0.77-0.81 (EPS). Autocorrelation (AR1) is low (<0.06) in all chronologies and Mean Sensitivity (MS) slightly lower in BS1650AB (0.48) compared to BS1650A and BS1650B (0.54). The SSS exceeds the 0.8 threshold since 1984 for chronologies A and AB and since 1996 for chronology B, limiting the common period of climate-growth analyses to 1996-2019 (Fig. 3).

3.2 Detection of partial rings

We estimated the rate of partial rings – expressed as the number of partial rings detected over 100 years – through the analysis of ring boundaries that have been digitized systematically with the help of high-resolution images obtained from microscope slide scanning. Detailed inspection of the 38 sections sampled from ind_{A-D} shows a mean rate of 34.3 partial rings per hundred years (sd = 14.7). Using different combi-

Tab. 1: Characteristics of the Bassiès *Rhododendron ferrugineum* detrended raw ring-width chronologies: length, sample depth (Nb.), mean series intercorrelation, rbar, EPS, the year in which the SSS 0.85 threshold is reached, first-order autocorrelation (AR1) and mean sensitivity (MS)

Chronology	Length	Nb.	Mean series intercorr	rbar	EPS	EPS (1996-2017)	Year SSS>0.8	AR1	MS
BS1650AB	1971-2019	15	0.42	0.25	0.78	0.85	1984	0.06	0.49
BS1650A	1971-2019	15	0.43	0.23	0.76	0.80	1984	0.06	0.54
BS1650B	1991-2019	15	0.33	0.19	0.77	0.77	1996	0.03	0.54

nations of one to four radii (a-d) on each section, we realize that 30 to 73% of the partial rings were detected on a single radius. The latter value was obtained using the longest radius (a) (Fig. 4). By measuring along two radii, more than 70% of the partial rings could be found (max. 88%) depending on the combination of radii used. Finally, using three radii, the median success rate systematically exceeds 90% and reaches 100% by combining radii a, b and d (Fig. 4).

3.3 Detection of missing rings

Amongst the 39 sections sampled from $ind_{A\text{-}D}$, 39% did not show any missing ring. The rate of missing rings was on average 4.53 missing rings per 100 years (Fig. 5A). Missing rings were more frequent in individuals A (6.63), B (2.03) and C (9.38) but significantly scarcer (0.46 missing rings per century) in individual D (Fig. 5A). The serial sectioning approach also showed that missing rings were rather evenly distributed along stems, even if the missing ring rate is slightly minimized (<3 missing years per century) when sections are sampled close to the soil surface rather than at 20 and 40 cm above the soil surface (>5 missing rings per century). Rates of missing rings also exceeded 10% in 6 out of 39 sections with maximum values (>15 rings per century) observed in sections from stems A1 and C1 (Fig. 5A). The ring of 2019 was, for instance, missing in 16 (42%) sections. Fig 5B shows that 27% of the total missing rings were missing for two or more consecutive years

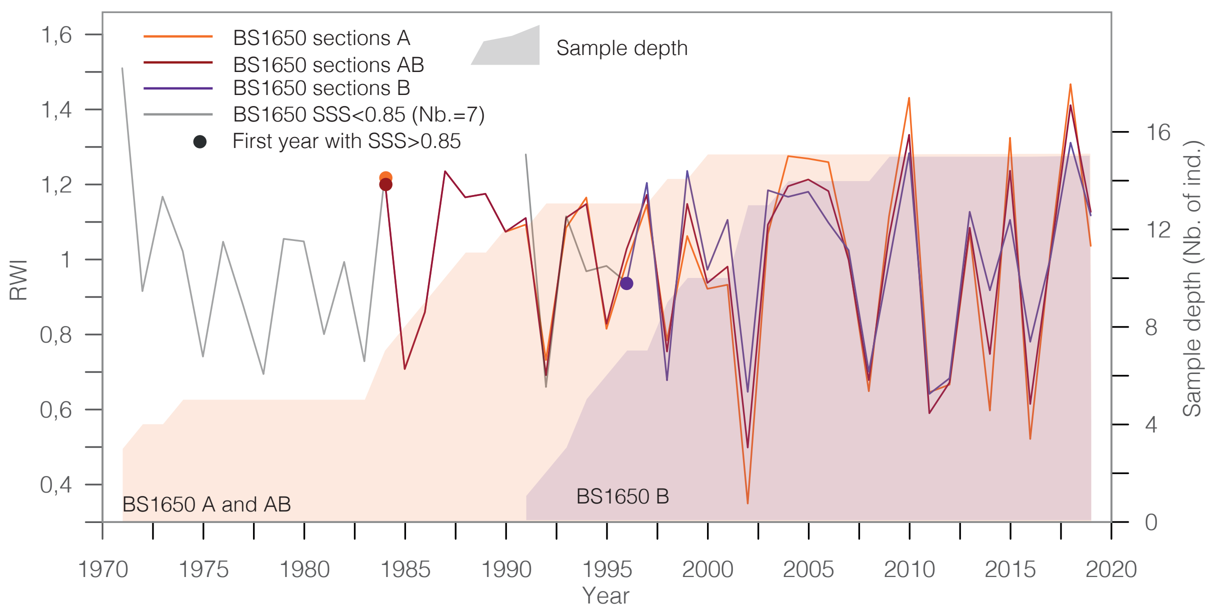

Fig. 3: Detrended *Rhododendron ferrugineum* ring-width chronologies based on base sections (BS1650A), stem sections (BS1650B), and both base and stem sections (BS1650AB). Sample size is indicated with colored background surfaces. Colored circles indicate the first year when the subsample signal strength (SSS) 0.85 threshold is reached. This threshold is always reached when seven individuals are added in the chronology.

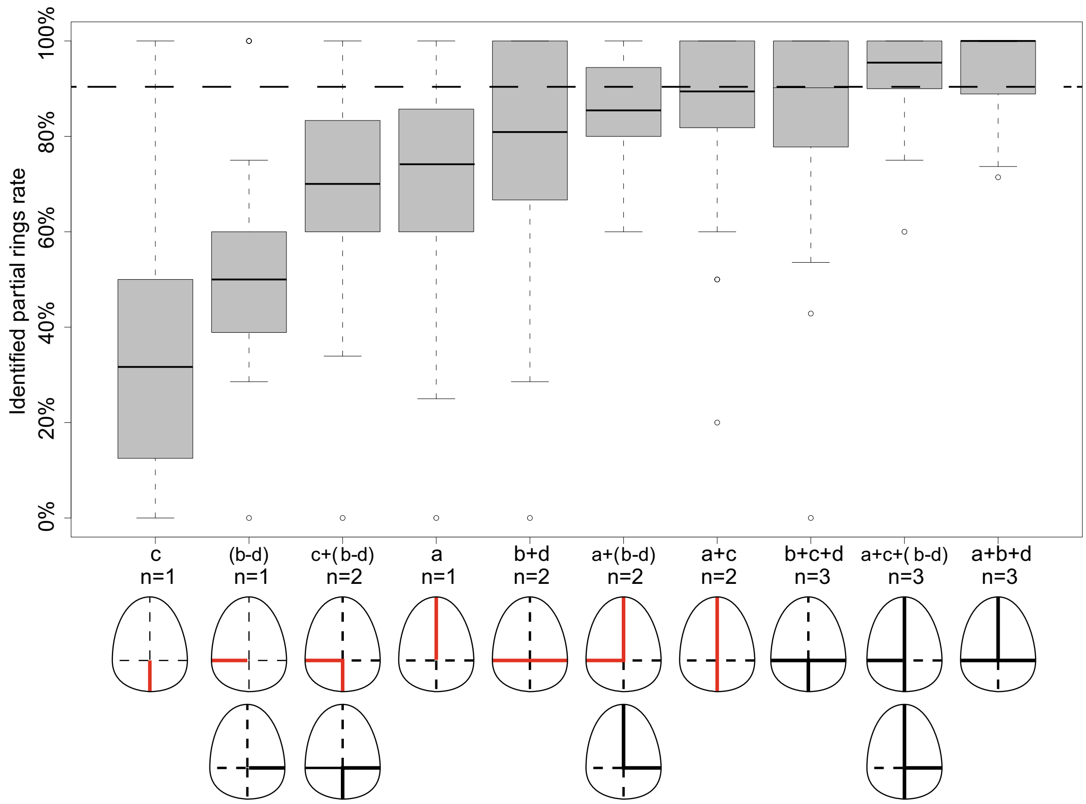

Fig. 4: Partial ring rates identified in individuals A, B, C and D by measuring growth rings at different radii. The different combinations are shown below the x-axis.

(e.g., A1.2 in 2015-2017), and that a ring missing for a given year was very often - although not systematically - missing at several heights along the stem. For instance, the ring of 2013 was missing in sections 3, 4, 5, and 7 in stem A1. Finally, Figure 5A shows that the sampling of an additional section 20 cm higher on the stem is sufficient to detect *c.* 75% of the missing rings that were present at the base. This percentage is not improved by adding more sections.

3.4 Intra-individual climate signal

Bootstrapped Correlation Functions (BCFs) between average monthly climate parameters and BS1650AB (Fig. 6A-D) show significant correlations between ring widths (RWI), minimum, mean and maximum July ($r=0.47$, $r=0.58$ and $r=0.58$, $p < 0.05$) and January temperature ($r=-0.37$, -0.45 and -0.58, $p < 0.05$) and previous minimum June temperature (0.59, $p<0.05$) over the period 1996-2017. We also found significant correlations between the BS1650AB chronology and previous September and December-February ($r = 36$ and $r = 0.47$, $p < 0.05$) precipitations totals and snowpack height (0.46, $p < 0.05$). The comparison of BCFs computed from BS1650A and BS1650B over the period 1996-2017 shows that BS1650A portrays the strongest summer temperature (both summer n and n-1) signal (Fig. 6ABC). For example, correlation coefficients with mean July temperature increase from 0.41 ($p>0.05$) for BS1650B to 0.59 ($p<0.05$) when using BS1650A as explained variable (Fig. 6D-E). Comparable significant negative correlations with winter temperatures are found with BS1650A compared to BS1650B. Conversely, a slightly higher winter (December to February) precipitation and snowpack height signal is extracted from BS1650B (Fig. 6D).

We computed a LMM using only significant monthly climate variables detected in the BCF analyses as fixed parameters, i.e., mean July temperature, minimum previous June temperature and snowpack height, interacting with the sample type (A or B). Maximum January temperature and winter precipitation were excluded because they showed too strong collinearity with snowpack height according to the VIF analysis. For the 1996-2017 period, the LMM

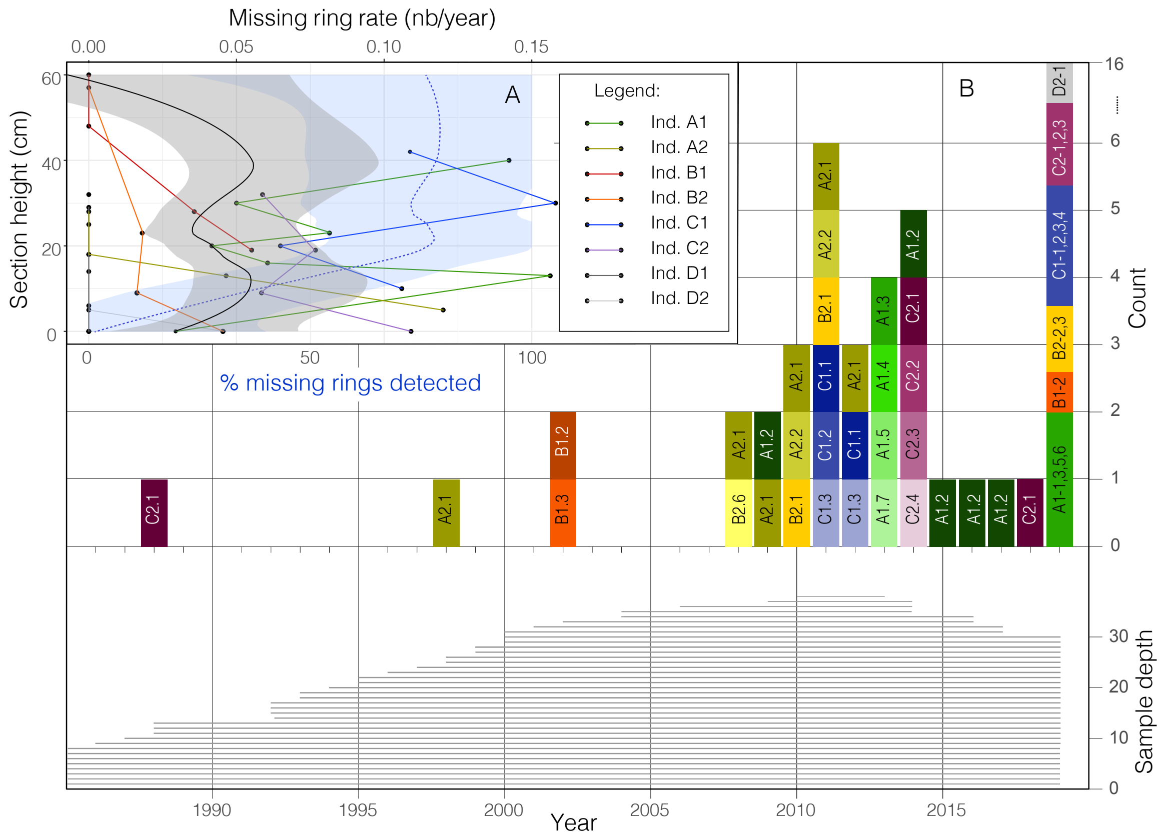

Fig. 5: (A) Missing ring rate according to section height in each stem of individuals A, B, C and D. The black line represents the loess regression. The grey ribbon indicates the 95% confidence interval. The blue dashed line represents the cumulative percentage of missing rings present at the base that were detected by adding sections higher in the stem (B) Number of missing rings in the chronology with each color corresponding to a specific stem and color gradient corresponding to the different sections within the stems. The y-axis had to be inflated for the year 2019 for which many missing rings have been detected. The sample depth of the sections is given below for reference.

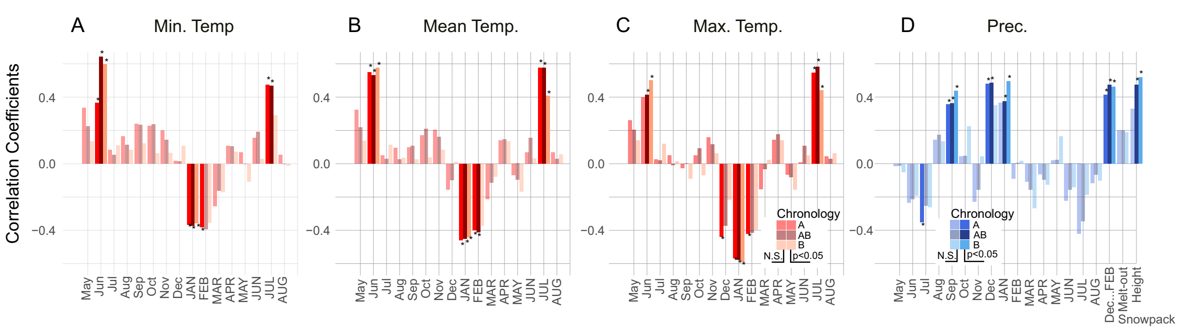

Fig. 6: (A, B, C, D) Bootstrapped correlation functions (BCFs) computed between the three chronologies and monthly (seasonal) precipitation sums (D) and average minimum, mean and maximum temperatures (A,B,C). Months of the year preceding ring formation are shown with lowercase letters. Bootstrapped Correlation Functions (BCFs) were computed over the period 1996-2017. Significant correlations (p<0.05) are indicated by an asterisk and darker colors.

showed a significantly higher sensitivity to the mean July temperature of the A sections compared to the B sections ($p < 0.01$, Tab. 2 and Fig. 7). However, we could not confirm effects of snowpack height, previous June temperature or interaction with section height as shown in the BCF analysis (Tab. 2 and Fig. 7).

Tab. 2: Significance of fixed effects (i.e. Jul T = July temperature, PDJF = winter precipitation totals and TJF = mean temperature in January and February) in the three linear mixed models computed over the period 1996-2017 showing the significance of interactions, indicating a difference in climate sensitivity depending on section height. Conditional R2 (R2c), marginal R2 (R2m), AIC and AIC differences between each model and a null model (ΔAIC_{null}) are given as well. NS = p > 0.05

Linear mixed model output		
$R^2m = 0.12$; $R^2c = 0.23$		
Parameter	Value and Signif.	t-value
Intercept	-0.07	-0.52
July Temp.	0.58***	3.91
Snowpack Height	-0.05	-0.34
Previous min. June Temp.	0.12	0.90
Section Height	0.02	0.32
Section Height * July Temp.	-0.28***	-3.51
Section Height * Snowpack Height	0.11	1.48
Section Height * Previous min. June Temp.	0.02	0.33

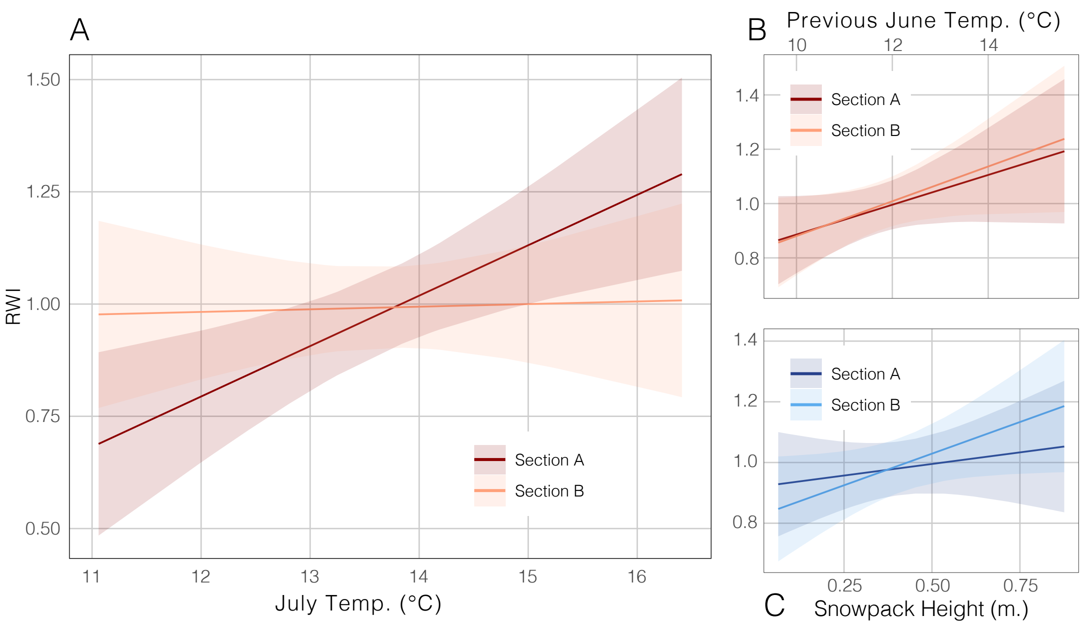

Fig. 7: Linear mixed models of *R. ferrugineum* detrended ring-width (RWI or ring-width index) as a function of July temperature, minimum previous June temperature and snowpack height, and their interaction with sections height (A: base and B: stems at 30 cm above soil surface) for the period 1996–2017. Solid lines and ribbons indicate the slope estimates and 95% confidence interval for the mixed model analyses.

4 Discussion

4.1 Chronology quality

The population we sampled is rather young (average age of 36 years), in line with shrub encroachment documented in the Bassiès valley and more generally in the Pyrenees since the late 1980s and as a result of both global warming and abandonment of pastoral practices (Galop et al. 2011, Szczypta et al. 2015). Rather low rbar and EPS values for all chronologies show relatively heterogeneous individual growth, which is common for shrubs (Buras 2017) due to fine-scale microhabitat, snowpack spatial heterogeneity (Ernakovich et al. 2014, Dobbert et al. 2022, Scherrer & Körner 2010, Weijers et al. 2018b) and complex resource allocation within stems (Buras & Wilmking 2017). However, such values are comparable to statistics obtained for *Rhododendron nivale* and *Rhododendron aganniphum* in the Himalayas (Liang & Eckstein 2009, LU et al. 2015) and certain *R. ferrugineum* chronologies used in Francon et al. (2021). Nevertheless, over the period used in this study for climate-growth analysis (1996-2019), statistics attest the robustness of the chronologies. Furthermore, the SSS statistics shows that the loss of explanatory power of the subsample due to decreasing sample size since 1996 is less than 20% for all chronologies.

4.2 Partial and missing ring detection

Cross-dating is a major issue in shrub dendrochronology due to the presence of ring patterns that are characterized by numerous partially or completely missing rings (Bär et al. 2006, 2008, Buras & Wilmking 2014, Hallinger et al. 2010, Keuper et al. 2012, Ropars et al. 2017). Here we used a serial sectioning approach (Kolishchuk 1990) – the recommended method in shrub dendrochronology (Bär et al. 2006, 2008, Buchwal et al. 2013, Buras & Wilmking 2014, Hallinger et al. 2010, Keuper et al. 2012, Liang et al. 2015, Liang & Eckstein 2009, Ropars et al. 2017) - to ensure precise detection of missing rings in *R. ferrugineum* individuals. Using a very dense serial sectioning along different stems in four individuals, we were able to identify all missing rings. However, in contrast to Kolishchuk (1990) and Wilmking et al. (2012) who showed that missing rings were less frequent in the juvenile part of dwarf trees, we did not detect such a trend in *R. ferrugineum.* On the contrary, our results demonstrate that several rings were absent along entire stems or individuals and were therefore challenging to be detected with a serial sectioning approach. In addition, most previous studies recommend sampling approximately 3 to 12 sections to detect missing rings within a single stem (Bär et al. 2006, Hallinger et al. 2010, Myers-Smith et al. 2015b, Shetti et al. 2018, Wilmking et al. 2012). In our case, we show that adding a single section to root collar is sufficient to detect the missing rings. Adding additional sections further up the stem does not help to improve the detection of missing rings.

Our study also confirms that partial (or wedging) rings are common features in ring patterns of multi-stemmed dwarf shrubs (Buras & Wilmking 2014). These discontinuous and incomplete rings result from failures in cambial activity (Myers-Smith et al. 2015a, Schweingruber & Poschlod 2005) and their detection requires either digitization of the ring boundaries (Buras & Wilmking 2014) or measurements of ring widths (RW) along different radii of a given section. The digitization of ring boundaries ensures that no partial ring is overlooked (Bär et al. 2006, Buras & Wilmking 2014, LI et al. 2013), but this method is extremely time-consuming. Our results show that measuring RW along three (including the largest) orthogonal radii allowed detect all the partial rings in most of the sampled sections. This means that one radius less than what was recommended by Buras & Wilmking (2014) for *J. communis* could suffice to detect partial rings on *R. ferrugineum.* This difference probably likely results from the structure of *R. ferrugineum* individuals forming concentric stems more frequently than *J. communis.* Consequently, and with the aim of optimizing the detection of missing rings in a time-saving manner, we can now recommend limiting the measurements of ring widths to three radii of each sampled *R. ferrugineum* section.

4.3 Climate-growth relationships

The three chronologies developed at our site (BS1650A, BS1650B, BS1650AB) showed comparable correlation profiles with monthly climatic parameters. Radial growth of *R. ferrugineum* at the study site was driven mainly by July temperature. Similarly, warmer temperatures during the growing season have been identified as key factors promoting shrub growth in different arctic and Alpine regions (e.g., Bär et al. 2008, Forbes et al. 2010, Francon et al. 2017, 2021, Hallinger et al. 2010, Myers-Smith et al. 2015a, Weijers et al. 2028b). In addition, significant correlations were computed between ring widths, winter precipitation, related snowpack height (positive) and mean maximum winter temperature (negative), thereby revealing the key influence of snowpack height on shrub ring productivity. Extremely narrow rings have been observed in *R. ferrugineum* individuals after dry winters characterized by shallow snowpack at low-elevation sites in the Alps (Francon et al. 2017, 2020a, 2023). Yet, the positive correlation observed between RWI and winter precipitation has not been reported so far in Alpine studies where thick and long-lasting snowpacks have negative effect on shrub growth through a shortening of the growing season (Carrer et al. 2019, Francon et al. 2017, 2020a). By contrast, our Pyrenean winter signal is in line with several studies in the Arctic and in Himalaya (LI et al. 2013, Liang et al. 2012, Zlatan & Gajewski 2006) where the positive response of radial growth to winter precipitation has been related to the protective thermal effect of snow against frost (Neuner 2014) and/or winter desiccation (Sakai & Larcher 1987). Such assumptions would be also valid at our site where *R. ferrugineum* is located at the lowermost limit of its ecological range (Escaravage et al. 1998). In fact, this species occurs preferentially in sheltered areas with a deep snowpack in winter (Körner 2003) and is therefore likely to suffer from an increasingly shallower and ephemeral snowpack at lower elevations and ongoing global warming. Average minimum previous June temperature is also determinant for shrub radial growth in our site. Once again, late-frost events during previous growing season could have detrimental effects on radial growth the following year through cellular damages on the cambium, buds, roots and leaves, or loss of hydraulic conductivity due to xylem cavitation (Charrier et al. 2017, Inouye et al. 2002, Komac et al. 2016). Besides the potential impact of late-frost, high photosynthesis rates in the year before ring formation could lead to high carbon storage and thus to increased growth in the following year (e.g., Babst et al. 2012, Francon et al. 2017, Fritts 1976). Yet, the effects of late frost on alpine shrub growth should be given greater consideration in future studies, especially for populations that are at the lower edge of the species' ecological niche.

4.4 Climate sensitivity along stems

The conventional approach in shrub dendroecology is to sample stem sections near the ground surface to increase the length of the ring width series (Myers-Smith et al. 2015b, Pellizzari et al. 2014, 2017, Ropars et al. 2017). However, and due to the generalization of the serial sectioning approach, sections sampled at different heights have often been averaged into individual series and subsequently into chronologies (Forbes et al. 2010, Francon et al. 2017, 2020b, 2020a, 2021, Hallinger et al. 2010, Hollesen et al. 2015, Liang et al. 2012). Such an aggregation was also justified by the fact that a unique section would not be sufficient to fully capture the response of a shrub to climate variables (Myers-Smith et al. 2015b, Shetti et al. 2018). Two recent studies were conducted with the purpose to unify sampling protocols, but could not agree on the number of sections to be included in a chronology to optimally extract the climate signal from shrub ring width series (Ropars et al. 2017, Shetti et al. 2018). Both studies agree that the inclusion of multiple sections from the same individual did not increase the climate signal. They also emphasized the need for more studies exploring the climate signal within stems in different shrub species.

Following these suggestions, we investigated the climate signal in three *R. ferrugineum* chronologies including cross-sections sampled at the base (BS1650A), 30 cm above the soil surface (BS1650B) and at both heights (BS16501AB). Both results from bootstrapped correlation functions and the linear mixed modelling approach show that BS1650A better preserves the summer temperature signal. Our findings thus are in line with results reported for *B. glandulosa* from northwestern Québec (Canada) (Ropars et al. 2017) for which sections taken at the root collar better represented climatic conditions as they encompassed the growth of the whole plant and as they were less subject to intraplant competition-like mechanisms. Results differed from findings reported for *J. communis* where temperature sensitivity did not vary significantly along the stem (Shetti et al. 2018). Regarding sensitivity to snowpack depth (highly related to winter precipitation and temperature in our analysis), we see slightly greater – although not significant - shrub sensitivity at 30 cm above the soil surface. We interpret this signal as lower protection of higher sections from extreme temperatures in winter and spring before melt-out. In addition, the minimum temperature signal in May-June (year n-1), which was detected uniformly along the stems, is likely an indirect and delayed physiological response. Thus, the growth response to the previous year's stress is reflected throughout the individual and not just in the most exposed parts of the stem.

5 Conclusions and implications for future sampling strategies

The study presented here provides guidance on how to design sampling that ensures accurate and efficient detection of missing rings in a multi-stemmed dwarf shrub species (*R. ferrugineum*) while maximizing the climate signal. We show that a serial sectioning approach based on solely two sections is sufficient to detect missing rings in the case of *R. ferrugineum* as (1) the rate of missing rings varied only slightly along shrub stems and (2) rings missing at the base were frequently missing along the entire stem. We therefore recommend developing *R. ferrugineum* chronologies following a two-steps procedure which involves successively (1) the averaging of cross-dated measurements made along three-radii from the same sections, (2) the averaging of two sections (at the stem base and around 20/30cm higher in the stem) for each individual. By selectively sampling two sections at different heights, we were also able to isolate and amplify two contrasting climate signals. Sections sampled at the shrub base provided better integration of July temperature fluctuations than stem-based or mixed chronologies. Higher stem sections were more sensitive to snow accumulation than shrub base sections. We hypothesize that differential exposure to frost events explains this divergent sensitivity to snowpack height. Although further investigations are required to (1) determine the degree to which these findings are generalizable to other shrub species in mountain environments and (2) to better understand the effects of frost, our results confirm that sampling design is crucial as it preconditions the success of dendroecological studies on shrubs.

Acknowledgments

This research was supported by the LabEx Driihm (*Dispositif de Recherche Interdisciplinaire sur les Interactions Hommes-Milieux*), INEE, CNRS, through the Shrub project. We thank the OHM Haut-Vicdessos Human-Environmental Observatory and its director, Didier Galop, for the financial support. We thank all who contributed to the meteorological series data used in the analyses, especially Samuel Morin (Météo-France - CNRS, CNRM, CEN). We are grateful to Lenka Slamova for her help during the laboratory phase.

References

Babst F, Carrer M, Poulter B, Urbinati C, Neuwirth B, Frank D (2012) 500 years of regional forest growth variability and links to climatic extreme events in Europe. *Environmental Research Letters* 7: 045705. https://doi.org/10.1088/1748-9326/7/4/045705

Bär A, Bräuning A, Löffler J (2006) Dendroecology of dwarf shrubs in the high mountains of Norway – A methodological approach. *Dendrochronologia* 24: 17–27. https://doi.org/10.1016/j.dendro.2006.05.001

Bär A, Pape R, Bräuning A, Löffler J (2008) Growth-ring variations of dwarf shrubs reflect regional climate signals in alpine environments rather than topoclimatic differences. *Journal of Biogeography* 35: 625–636. https://doi.org/10.1111/j.1365-2699.2007.01804.x

Bartoń K (2019) MuMIn: Model selection and model averaging based on information criteria (AICc and alike)(R Package Version, 1–1, 2014)

Buchwal A (2014) Constraints on dendrochronological dating of Salix polaris from central Spitsbergen (Short communication). *Czech Polar Reports* 4: 73–79. https://doi.org/10.5817/CPR2014-1-8

Buchwal A, Rachlewicz G, Fonti P, Cherubini P, Gärtner H (2013) Temperature modulates intra-plant growth of Salix polaris from a high Arctic site (Svalbard). *Polar Biology* 36: 1305–1318. https://doi.org/10.1007/s00300-013-1349-x

Bunn AG (2008) A dendrochronology program library in R (dplR). *Dendrochronologia* 26: 115–124. https://doi.org/10.1016/j.dendro.2008.01.002

Buras A (2017) A comment on the expressed population signal. *Dendrochronologia* 44: 130–132. https://doi.org/10.1016/j.dendro.2017.03.005

Buras A, Wilmking M (2014) Straight lines or eccentric eggs? A comparison of radial and spatial ring width measurements and its implications for climate transfer functions. *Dendrochronologia* 32: 313–326. https://doi.org/10.1016/j.dendro.2014.07.002

Carrer M, Pellizzari E, Prendin AL, Pividori M, Brunetti M (2019) Winter precipitation - not summer temperature - is still the main driver for Alpine shrub growth. *Science of The Total Environment* 682: 171–179. https://doi.org/10.1016/j.scitotenv.2019.05.152

Chapin FS et al. (2005) Role of Land-surface changes in Arctic summer warming. *Science* 310: 657–660. https://doi.org/10.1126/science.1117368

Charrier G, Nolf M, Leitinger G, Charra-Vaskou K, Losso A, Tappeiner U, Améglio T, Mayr S (2017) Monitoring of freezing dynamics in trees: A simple phase shift causes complexity. *Plant Physiology* 173: 2196–2207. https://doi.org/10.1104/PP.16.01815

Cook ER, Peters K (1981) The smoothing spline: A new approach to standardizing forest interior tree-ring width series for dendroclimatic studies. *Tree ring bulletin*. 41: 45–53.

Delmas M, Calvet M, Gunnell Y, Braucher R, Bourlès D (2011) Palaeogeography and 10Be exposure-age chronology of Middle and Late Pleistocene glacier systems in the northern Pyrenees: Implications for reconstructing regional palaeoclimates. *Palaeogeography, Palaeoclimatology, Palaeoecology* 305: 109–122. https://doi.org/10.1016/j.palaeo.2011.02.025

Dobbert S, Pape R., Löffler J (2022). On growth patterns and mechanisms in arctic-alpine shrubs. *Erdkunde* 76: 199–226. https://doi.org/10.3112/erdkunde.2022.03.04

Durand Y, Giraud G, Laternser M, Etchevers P, Mérindol L, Lesaffre B (2009) Reanalysis of 47 years of climate in the French Alps (1958–2005): Climatology and trends for snow cover. *Journal of Applied Meteorology and*

Climatology 48: 2487–2512. https://doi.org/10.1175/2009JAMC1810.1

Escaravage N, Questiau S, Pornon A, Doche B, Taberlet P (1998) Clonal diversity in a Rhododendron ferrugineum L. (Ericaceae) population inferred from AFLP markers. *Molecular Ecology* 7: 975–982. https://doi.org/10.1046/j.1365-294x.1998.00415.x

Ernakovich JG, Hopping KA, Berdanier AB, Simpson RT, Kachergis EJ, Steltzer H, Wallenstein MD (2014) Predicted responses of arctic and alpine ecosystems to altered seasonality under climate change. *Global Change Biology* 20: 3256–3269. https://doi.org/10.1111/gcb.12568

Forbes BC, Fauria MM, Zetterberg P (2010) Russian Arctic warming and 'greening' are closely tracked by tundra shrub willows. *Global Change Biology* 16: 1542–1554. https://doi.org/10.1111/j.1365-2486.2009.02047.x

Francon L, Corona C, Till-Bottraud I, Choler P, Carlson BZ, Charrier G, Améglio T, Morin S, Eckert N, Roussel E, Lopez-Saez J, Stoffel M (2020a) Assessing the effects of earlier snow melt-out on alpine shrub growth: The sooner the better? *Ecological Indicators* 115: 106455. https://doi.org/10.1016/j.ecolind.2020.106455

Francon L, Corona C, Roussel E, Lopez Saez J, Stoffel M (2017) Warm summers and moderate winter precipitation boost Rhododendron ferrugineum L. growth in the Taillefer massif (French Alps). *Science of The Total Environment* 586: 1020–1031. https://doi.org/10.1016/j.scitotenv.2017.02.083

Francon L, Corona C, Till-Bottraud I, Carlson BZ, Stoffel M (2020b) Some (do not) like it hot: Shrub growth is hampered by heat and drought at the alpine treeline in recent decades. *American Journal of Botany* 107: 607–617. https://doi.org/10.1002/ajb2.1459

Francon L, Corona C, Till-Bottraud I, Choler P, Roussel E, Carlson BZ, Morin S, Girard B, Stoffel M (2021) Shrub growth in the Alps diverges from air temperature since the 1990s. *Environmental Research Letters* 16: 074026. https://doi.org/10.1088/1748-9326/ac0b67

Francon L, Roussel E, Lopez-Saez J, Saulnier M, Stoffel M, Corona C (2023) Alpine shrubs have benefited more than trees from 20th century warming at a treeline ecotone site in the French Pyrenees. *Agricultural and Forest Meteorology* 329: 109284. https://doi.org/10.1016/j.agrformet.2022.109284

Fritts HC (1976) Tree rings and climate. London , New York

Galop D, Houet T, Mazier F, Leroux G, Rius D (2011) Grazing activities and biodiversity history in the Pyrénées - new insights on high altitude ecosystems in the framework of a human-environment observatory. *Pages News* 19: 53. https://pastglobalchanges.org/publications/pages-magazines/pages-magazine/7531

Hallinger M, Manthey M, Wilmking M (2010) Establishing a missing link: warm summers and winter snow cover promote shrub expansion into alpine tundra in Scandinavia. *New Phytologist* 186: 890–899. https://doi.org/10.1111/j.1469-8137.2010.03223.x

Hallinger M, Wilmking M (2011) No change without a cause – why climate change remains the most plausible reason for shrub growth dynamics in Scandinavia. *New Phytologist* 189: 902–908. https://doi.org/10.1111/j.1469-8137.2010.03624.x

Hollesen J, Buchwal A, Rachlewicz G, Hansen BU, Hansen MO, Stecher O, Elberling B (2015) Winter warming as an important co-driver for Betula nana growth in western Greenland during the past century. *Global Change Biology* 21: 2410–2423. https://doi.org/10.1111/gcb.12913

Inouye DW, Morales MA, Dodge GJ (2002) Variation in timing and abundance of flowering by Delphinium barbeyi Huth (Ranunculaceae): The roles of snowpack, frost, and La Niña, in the context of climate change. *Oecologia* 130: 543–550. https://doi.org/10.1007/s00442-001-0835-y

IPCC (2021) Climate change 2021: The physical science basis. Contribution of Working Group I to the Sixth Assessment Report of the Intergovernmental Panel on Climate. Cambridge, New York. https://doi.org/10.1017/9781009157896

Keuper F, Parmentier F-JW, Blok D, Van Bodegom PM, Dorrepaal E, Van Hal JR, Van Logtestijn RSP, Aerts R (2012) Tundra in the rain: Differential vegetation responses to three years of experimentally doubled summer precipitation in Siberian shrub and Swedish bog tundra. *Ambio* 41: 269–280. https://doi.org/10.1007/s13280-012-0305-2

Kolishchuk V (1990) Dendroclimatological study of prostrate woody plant. Cook ER, Kairiukstis LA (eds) *Methods of Dendrochronology - Applications in the environmental sciences:* 51–55. Dordrecht.

Komac B, Esteban P, Trapero L, Caritg R (2016) Modelization of the current and future habitat suitability of Rhododendron ferrugineum using potential snow accumulation. *Plos One* 11: e0147324. https://doi.org/10.1371/journal.pone.0147324

Körner C (2003) Alpine plant life: Functional plant ecology of high mountain ecosystems. Berlin, Heidelberg.

Li Z, Liu G, FU B, Zhang Q, MA K, Pederson N (2013) The growth-ring variations of alpine shrub Rhododendron przewalskii reflect regional climate signals in the alpine environment of Miyaluo Town in Western Sichuan Province, China. *Acta Ecologica Sinica* 33: 23–31. https://doi.org/10.1016/j.chnaes.2012.12.004

Liang E, Eckstein D (2009) Dendrochronological potential of the alpine shrub Rhododendron nivale on the south-eastern Tibetan Plateau. *Annals of Botany* 104: 665–670. https://doi.org/10.1093/aob/mcp158

Liang E, Liu W, Ren P, Dawadi B, Eckstein D (2015) The alpine dwarf shrub Cassiope fastigiata in the Himalayas:

does it reflect site-specific climatic signals in its annual growth rings? *Trees* 29: 79–86. https://doi.org/10.1007/s00468-014-1128-5

Liang E, LU X, Ren P, LI X, Zhu L, Eckstein D (2012) Annual increments of juniper dwarf shrubs above the tree line on the central Tibetan Plateau: A useful climatic proxy. *Annals of Botany* 109: 721–728. https://doi.org/10.1093/aob/mcr315

Liston GE, Mcfadden JP, Sturm M, Pielke RA (2002) Modelled changes in arctic tundra snow, energy and moisture fluxes due to increased shrubs. *Global Change Biology* 8: 17–32. https://doi.org/10.1046/j.1354-1013.2001.00416.x

Lu X, Camarero JJ, Wang Y, Liang E, Eckstein D (2015) Up to 400-year-old *Rhododendron* shrubs on the southeastern Tibetan Plateau: Prospects for shrub-based dendrochronology. *Boreas* 44: 760–768. https://doi.org/10.1111/bor.12122

Marti R, Gascoin S, Berthier E, De Pinel M, Houet T, Laffly D (2016) Mapping snow depth in open alpine terrain from stereo satellite imagery. *The Cryosphere* 10: 1361–1380. https://doi.org/10.5194/tc-10-1361-2016

Moullec ML, Buchwal A, Wal R Van Der, Sandal L, Hansen BB (2019) Annual ring growth of a widespread high arctic shrub reflects past fluctuations in community-level plant biomass. *Journal of Ecology* 107: 436–451. https://doi.org/10.1111/1365-2745.13036

Myers-Smith IH et al. (2011) Shrub expansion in tundra ecosystems: dynamics, impacts and research priorities. *Environmental Research Letters* 6: 045509. https://doi.org/10.1088/1748-9326/6/4/045509

Myers-Smith IH et al. (2015a) Climate sensitivity of shrub growth across the tundra biome. *Nature Climate Change* 5: 887–891. https://doi.org/10.1038/nclimate2697

Myers-Smith IH et al. (2015b) Methods for measuring arctic and alpine shrub growth: A review. *Earth-Science Reviews* 140: 1–13. https://doi.org/10.1016/j.earscirev.2014.10.004

Myers-Smith IH et al. (2020) Complexity revealed in the greening of the Arctic. *Nature Climate Change* 10, 106–117. https://doi.org/10.1038/s41558-019-0688-1

Nakagawa S, Schielzeth H (2013) A general and simple method for obtaining R^2 from generalized linear mixed-effects models. *Ecology and Evolution* 4: 133–142. https://doi.org/10.1111/j.2041-210x.2012.00261.x

Neuner G (2014) Frost resistance in alpine woody plants. *Frontiers in Plant Science* 5: 654. https://doi.org/10.3389/fpls.2014.00654

Pellizzari E, Camarero JJ, Gazol A, Granda E, Shetti R, Wilmking M, Moiseev P, Pividori M, Carrer M (2017) Diverging shrub and tree growth from the Polar to the Mediterranean biomes across the European continent. *Global Change Biology* 23: 3169–3180. https://doi.org/10.1111/gcb.13577

Pellizzari E, Pividori M, Carrer M (2014) Winter precipitation effect in a mid-latitude temperature-limited environment: the case of common juniper at high elevation in the Alps. *Environmental Research Letters* 9: 104021. https://doi.org/10.1088/1748-9326/9/10/104021

Piccinelli S, Francon L, Corona C, Slamova L, Cannone N (2023). Vessels in a Rhododendron ferrugineum (L.) population do not trace temperature anymore at the alpine shrubline. *Frontiers in Plant Science* 13. 1023384. https://doi.org/10.3389/fpls.2022.1023384

R Core Team (2016) R: A language and environment for statistical computing. R Foundation for Statistical Computing. Vienna.

Ropars P, Angers-Blondin S, Gagnon M, Myers-Smith IH, Lévesque E, Boudreau S (2017) Different parts, different stories: Climate sensitivity of growth is stronger in root collars vs. stems in tundra shrubs. *Global Change Biology* 23: 3281–3291. https://doi.org/10.1111/gcb.13631

Sakai A, Larcher W (1987) Low temperature and frost as environmental factors. Sakai A, Larcher W (eds) *Frost survival of plants: Responses and adaptation to freezing stress*: 1–20. Berlin, Heidelberg.

Scherrer D, Körner C (2010) Topographically controlled thermal-habitat differentiation buffers alpine plant diversity against climate warming. *Journal of Biogeography* 38: 406–416. https://doi.org/10.1111/j.1365-2699.2010.02407.x

Schweingruber FH, Poschlod P (2005) Growth rings in herbs and shrubs: Life span, age determination and stem anatomy. *Forest Snow and Landscape Research* 79:195–415.

Shetti R, Buras A, Smiljanic M, Wilmking M (2018) Climate sensitivity is affected by growth differentiation along the length of Juniperus communis L. shrub stems in the Ural Mountains. *Dendrochronologia* 49: 29–35. https://doi.org/10.1016/j.dendro.2018.02.006

Simonneau A et al (2013) Recent climatic and anthropogenic imprints on lacustrine systems in the Pyrenean Mountains inferred from minerogenic and organic clastic supply (Vicdessos valley, Pyrenees, France). *The Holocene* 23: 1764–1777. https://doi.org/10.1177/0959683613505340

Sturm M, Holmgren J, Mcfadden JP, Liston GE, Chapin FS, Racine CH (2001) Snow–shrub interactions in Arctic tundra: A hypothesis with climatic implications. *Journal of Climate* 14: 336–344. https://doi.org/10.1175/1520-0442(2001)014<0336:SSIAT>2.0.CO;2

Szczypta C, Calvet J-C, Maignan F, Dorigo W, Baret F, Ciais P (2014) Suitability of modelled and remotely sensed essential climate variables for monitoring Euro-Mediterranean droughts. *Geoscientific Model Development* 7: 931–946. https://doi.org/10.5194/gmd-7-931-2014

Szczypta C, Gascoin S, Houet T, Hagolle O, Dejoux J-F, Vigneau C, Fanise P (2015) Impact of climate and land cover changes on snow cover in a small Pyrenean catchment. *Journal of Hydrology* 521: 84–99. https://doi.org/10.1016/j.jhydrol.2014.11.060

Tape KD, Hallinger M, Welker JM, Ruess RW (2012) Landscape heterogeneity of shrub expansion in Arctic Alaska. *Ecosystems* 15: 711–724. https://doi.org/10.1007/s10021-012-9540-4

Vernay M, Lafaysse M Monteiro D, Hagenmuller P, Nheili R, Samacoïts R, Verfaillie D, Morin S (2022): The S2M meteorological and snow cover reanalysis over the French mountainous areas: description and evaluation (1958–2021). *Earth System Science Data* 14: 1707–1733. https://doi.org/10.5194/essd-14-1707-2022

Vionnet V, Brun E, Morin S, Boone A, Faroux S, LE Moigne P, Martin E, Willemet J-M (2012) The detailed snowpack scheme Crocus and its implementation in Surfex v7.2. *Geoscientific Model Development* 5: 773–791. https://doi.org/10.5194/gmd-5-773-2012

Weijers S, Broekman RA, Rozema J (2010) Dendrochronology in the High Arctic: July air temperatures reconstructed from annual shoot length growth of the circumarctic dwarf shrub Cassiope tetragona. *Quaternary Science Reviews* 29: 3831–3842. https://doi.org/10.1016/j.quascirev.2010.09.003

Weijers S, Beckers N, Löffler J (2018a) Recent spring warming limits near-treeline deciduous and evergreen alpine dwarf shrub growth. *Ecosphere* 9: e02328. https://doi.org/10.1002/ecs2.2328

Weijers S, Myers-Smith I H, Löffler J (2018b). A warmer and greener cold world: Summer warming increases shrub growth in the alpine and high arctic tundra. *Erdkunde* 72: 63–85. https:// doi.org/10.3112/erdkunde.2018.01.04

Wigley TML, Briffa KR, Jones PD (1984) On the average value of correlated time series, with applications in dendroclimatology and hydrometeorology. *Journal of Applied Meteorology and Climatology* 23: 201–213. https://doi.org/10.1175/1520-0450(1984)023<0201:Otavoc>2.0.CO;2

Wilmking M, Hallinger M, Van Bogaert R, Kyncl T, Babst F, Hahne W, Juday GP, DE Luis M, Novak K, Völlm C (2012) Continuously missing outer rings in woody plants at their distributional margins. *Dendrochronologia* 30: 213–222. https://doi.org/10.1016/j.dendro.2011.10.001

Zalatan R, Gajewski K (2006) Dendrochronological potential of Salix alaxensis from the Kuujjua River Area, Western Canadian Arctic. *Tree-Ring Research* 62: 75–82. https://doi.org/10.3959/1536-1098-62.2.75

Zang C, Biondi F (2015) treeclim: An R package for the numerical calibration of proxy-climate relationships. *Ecography* 38: 431–436. https://doi.org/10.1111/ecog.01335

Zuur AF, Ieno EN, Elphick CS (2010) A protocol for data exploration to avoid common statistical problems. *Methods in Ecology and Evolution* 1: 3–14. https://doi.org/10.1111/j.2041-210X.2009.00001.x

Authors

Tania Pereira
tania.pereira@unige.ch
Dr. Loïc Francon
ORCID: 0000-0002-2894-9774
loic.francon@unige.ch
University of Geneva
Institute for Environmental Sciences
Climate Change Impacts and Risks
in the Anthropocene (C-CIA)
66 Boulevard Carl Vogt
1205 Geneva
Switzerland

Dr. Christophe Corona
ORCID: 0000-0002-7645-6157
christophe.corona@unige.ch
University of Geneva
Institute for Environmental Sciences
Climate Change Impacts and Risks
in the Anthropocene (C-CIA)
66 Boulevard Carl Vogt
1205 Geneva
Switzerland
and
Université Clermont Auvergne
CNRS
Geolab
F-63000 Clermont-Ferrand
France

Prof. Dr. Markus Stoffel
ORCID: 0000-0003-0816-1303
markus.stoffel@unige.ch
University of Geneva
Institute for Environmental Sciences
Climate Change Impacts and Risks
in the Anthropocene (C-CIA)
and
Department of Earth Sciences
and
Department F.-A. Forel for
Environmental and Aquatic Science
66 Boulevard Carl Vogt
1205 Geneva
Switzerland